Two-Particle Correlations from Neutron–Light-Charged-Particle Coincidences

R. A. Kryger, J. J. Kolata, W. Chung, S. Dixit, R. J. Tighe, and J. J. Vega
Physics Department, University of Notre Dame, Notre Dame, Indiana 46556

P. A. DeYoung, C. Copi, and J. Sarafa
Physics Department, Hope College, Holland, Michigan 49423

D. G. Kovar
Physics Division, Argonne National Laboratory, Argonne, Illinois 60439

G. P. Gilfoyle and S. K. Sigworth
Department of Physics, University of Richmond, Richmond, Virginia 23173
(Received 13 Junc 1990)

The first correlation functions from a neutron–light-charged-particle small-angle coincidence measurement are reported for the $^{16}O+^{27}Al$ reaction at $E(^{16}O)=215$ MeV. Clear evidence for singlet-deuteron and ^{5}He production, and an anticorrelation of low-relative-momentum neutron-deuteron pairs, is observed. The nuclear temperature of 1.6 ± 0.3 MeV, calculated from the ratio of excited-state to ground-state deuteron emission and corrected for sequential emission, is considerably lower than expected.

PACS numbers: 25.70.Gh

In recent years, two-particle correlation data at small relative momenta have been used to probe properties of nuclear interactions such as source sizes,[1] temperatures,[2] and decay lifetimes.[3–5] Correlations resulting from interactions between the two emitted particles can arise from several sources, including nuclear and Coulomb final-state interactions,[6] decays of particle-unstable states,[7] and quantum statistics.[8] We report here on correlation functions measured in the first two-particle interferometry experiment involving neutron–light-charged-particle pairs, for which Coulomb interactions are absent. One principal motivation for this experiment was to test the "deuteron thermometer,"[9] the simplest of the quantum thermometers which register the temperature of nuclear systems in terms of the population ratio of excited states of thermally emitted particles. Measurements of this kind have been made for relatively long-lived, γ-emitting final states,[10] and also for particle-unbound states of complex fragments.[2] The deuteron thermometer is, however, particularly simple since the deuteron possesses only one excited state. It can also be utilized at lower energies where the thermal emission of more complex fragments is improbable, and where the reaction mechanism is more likely to involve the formation of an equilibrated compound nucleus. We will present *np*, *nd*, and *nα* correlation functions, the production cross sections for excited-state deuterons (d^*) and ^{5}He fragments, and the nuclear temperature deduced from the deuteron thermometer.

The experiment was performed using a 215-MeV ^{16}O beam from the ATLAS accelerator at Argonne National Laboratory incident on a 800-μg/cm^2 target of ^{27}Al. This reaction was selected since the equivalent charged-particle correlation data already exist.[5] Coincident particles were detected in two detector arrays centered at $\pm45°$ with respect to the beam and covering the angular range from 42° to 48°. Each array consisted of three NaI(Tl) charged-particle detectors in the horizontal plane, and four liquid-scintillator neutron detectors, two above and two below the horizontal plane. The opening angle between nearest neutron–charged-particle detector pairs was 3.1°. The six charged-particle detectors, 5.0-cm-diameter-by-3.8-cm-long cylindrical NaI(Tl) crystals covered with protective 6-mg/cm^2 Havar foils and coupled to phototubes, were placed 1.2 m from the target and collimated to a diameter of 3.8 cm. Charged-particle identification was accomplished off line using the energy, time-of-flight (TOF), and pulse-shape signals as described in Refs. 11 and 12, and energy calibrations for $Z=1$ and 2 particles were obtained via the $^{12}C(^{16}O,\alpha)$ reaction at several beam energies and the kinematics of ^{6}Li breakup. The eight neutron detectors, 12.5-cm-diameter-by-7.5-cm-long cylindrical NE-213 cells coupled to fast-timing phototubes, were placed 2.4 m from the target. Neutron shadowbars consisting of 25-cm-long brass cylinders placed halfway between the detector and the target were used to measure coincidence events due to scattered neutrons. Contaminant γ rays were removed off line by pulse-shape discrimination, and neutron energies were determined from the TOF. The time resolution of 1.0 ns, combined with the long neutron flight path, yielded excellent neutron energy resolution. The low-energy thresholds for each particle type were 2.0, 2.5, 2.7, and 6.6 MeV for *n*, *p*, *d*, and α particles, respectively, corresponding to the lowest energy where reliable particle identification could be made. The ^{16}O

beam consisted of approximately 260-ps-wide bunches (FWHM) separated by 240 ns, with an average current of 5 particle nA on target. Beam passing through the target was collected in a well shielded beam dump 4 m from the target. The total (dead-time-corrected) integrated charge on target was 5.3 mC.

Twofold neutron–light-charged-particle events were histogrammed according to the magnitude of the relative momentum q defined by

$$\mathbf{q}=\mu|\mathbf{v}_1-\mathbf{v}_2|\,.$$

The particle energies and detector angles determine the velocity vectors $\mathbf{v}_1$ and $\mathbf{v}_2$, and μ is the reduced mass of the coincident particles. Scattered-neutron coincidence events, measured in the shadowbar runs and normalized to the integrated charge on target, as well as random coincidences determined from events with particles from consecutive beam bursts, were subtracted from the measured q spectra. Correlation functions were then formed by taking the ratio of the measured relative momentum spectrum to a background spectrum which is free of correlations. We estimated this background for each two-particle combination by event mixing[13] the coincident events from the same pair of detectors, thus preserving all the detector characteristics and especially the thresholds and detection efficiencies. Furthermore, the small- (large-) opening-angle background is constructed from events with small (large) opening angles.

Figure 1 shows the correlation functions for the *np*, *nd*, and *nα* coincidence data obtained in the present experiment. The high-q data, indicated by squares in the figure, result from coincidences between particles detected on opposite sides of the beam (large-opening-angle events). These events are relatively free of correlations due to two-particle interactions and the correlation functions are flat and average to unity as expected. The low-q data, corresponding to coincident particles detected at small opening angles within the same detector array and indicated by circles in the figure, are most sensitive to two-particle correlations. Event-mixing uncorrelated data results in a self-normalized background so that all three correlation functions average to unity at high q. However, in the presence of strong positive (or negative) correlations such as occur in the *np* and *nα* (*nd*) small-opening-angle data, conservation of the number of events in the event-mixing procedure results in a constant overestimation (underestimation) of the background spectrum over the entire low-q region. This drives the local background correlation ratio below (above) unity. Thus the two peaks in the *np* and *nα* data are superimposed onto a flat local background that averages to 0.90 ± 0.03, 0.82 ± 0.03, and 1.04 ± 0.07 for the *np*, *nα*, and *nd* data, respectively. These values (shown by the dashed horizontal lines in Fig. 1) were determined by averaging the small-opening-angle correlation data away from the peaks (dip).

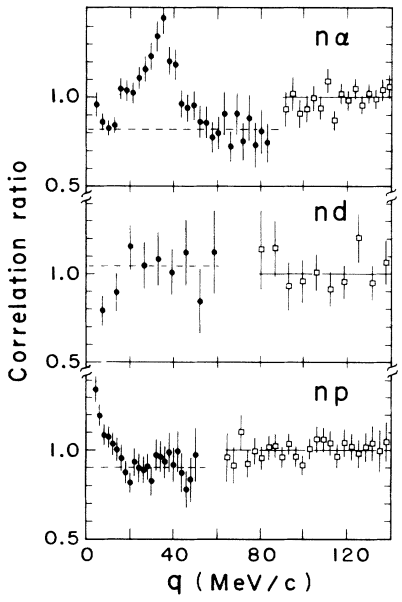

FIG. 1. Correlation functions for *nα*, *nd*, and *np* coincident events. Small-opening-angle data are indicated by circles and large-opening-angle data by squares. The dashed and solid horizontal lines indicate the background correlation ratio for the small- and large-opening-angle data as explained in the text.

The peaks in the *np* and *nα* correlation functions are due to the emission of particle-unstable states, specifically ^1S deuteron (d^*) emission in the *np* case and ^{5}He emission in the *nα* case. The *nd* correlation function is essentially flat due to the absence of particle-unstable states in the ^{3}H system, but with evidence for an anticorrelation at low-relative-momentum. This anticorrelation cannot be a Coulomb effect as there is no final-state Coulomb interaction between these two particles. One possibility is the reduction in low relative momentum *nd* pairs due to ground-state ^{3}H formation.[14] On the other hand, the observed anticorrelation may be due to the strongly repulsive *nd* quartet s-wave interaction, the nature of which is of considerable current interest[15,16] in three-body scattering theory. Very recently, it has been shown[16] to be a manifestation of the repulsion induced by the Pauli principle, in which case our anticorrelation would be a quantum-statistical effect.

Figure 2 shows the emission spectra for d^* and ^{5}He particles, extracted from the small-opening-angle coincidence data by renormalizing the event-mixed background spectrum (as discussed above) and subtracting the result from the measured relative momentum spectra. These data have been efficiency corrected by the effective solid angle for detection of correlated particle pairs. This efficiency, a function of the relative momentum and the individual detector thresholds, efficiencies, and solid angles, was determined from Monte Carlo simulations of d^* and ^{5}He emission from a ^{43}Sc compound nucleus. The laboratory energy distributions for

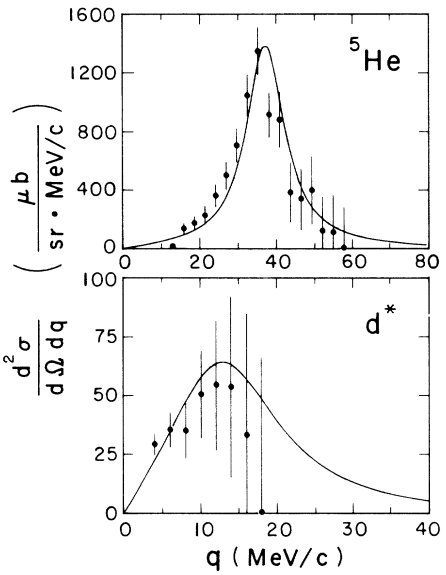

FIG. 2. Efficiency-corrected emission spectra for ^{5}He and d^*. The curves, which are normalized to the data, are explained in the text.

the d^* and ^{5}He particles were taken to be identical to the deuteron and α-particle spectra measured in this experiment. Energy-dependent neutron detector efficiencies determined from the program[17,18] TOTEFF were also incorporated into the simulation. The smooth curves in Fig. 2 are theoretical emission spectra in relative momentum for the two particle-unstable states, taken from the relative energy parametrizations of Ref. 7 converted to relative momentum and normalized to our data. We observe excellent agreement for the ^{5}He yield curve, and very good agreement for the d^* yield although the low detection efficiency for pn relative momenta above 20 MeV/c prevented us from observing d^* events in this region.

The cross sections for ^{5}He and d^* production were determined by integrating the curves in Fig. 2, giving 24 ± 2 mb/sr for ^{5}He production, and 1.3 ± 0.4 mb/sr for d^* production, at an average laboratory angle of 45°. The quoted errors do not reflect systematic uncertainties such as those incurred in the efficiency correction. The principle unknown in the efficiency correction (the calculated neutron detector response) is estimated to contribute less than 25% uncertainty. For comparison purposes, the measured cross sections for p, d, and α emission in this same experiment at $\Theta_{lab}=45°$ are 349 ± 1, 73.0 ± 0.5, and 477 ± 1 mb/sr, respectively.

Within the thermal model of composite particle emission,[19] the nuclear temperature is obtained from the ratio of d^* to d emission, R, which is related to the nuclear temperature and the energy difference of the two states according to

$$R=f\left(\frac{2J_1+1}{2J_2+1}\right)\exp\left(-\frac{\varepsilon}{T}\right).$$

Here, J_1 and J_2 are the spins of the d and d^*, respectively, ε is the energy separation between the two states ($\varepsilon=2.26$ MeV), and T is the nuclear temperature in MeV. The quantity f is a phase-space factor that reduces the emission probability for virtual states such as the d^* and for broad resonances.[20] In the present case, $f=0.34$. The experimental d^*/d ratio gives $T=1.2\pm0.3$ MeV, considerably lower than the temperatures suggested by the slopes of the light-particle (n,p,d,α) emission spectra, all of which are above 4 MeV. Even the d^* emission spectrum, obtained by summing the c.m. energy of the detected proton and neutron (deduced from the laboratory energies assuming emission from the compound nucleus), gives a slope temperature consistent with that obtained from the other light-particle spectra. This low d^*/d temperature, relative to the slope temperatures, is similar to the results of previous population ratio temperature measurements[2,10,21] using heavier mass fragments.

The nuclear temperature of the ^{43}Sc compound system, including a correction for excitation energy bound up in collective motion, can be calculated in the Fermi-gas model.[22] We compute an average nuclear temperature of 4.4 MeV from the temperatures of the daughter nuclei produced in the deexcitation of the ^{43}Sc system [as predicted by CASCADE (Ref. 23)], weighted by the deuteron emission probability of each daughter. This is considerably hotter than the d^*/d result but in good agreement with the slope temperatures. Although there are no higher-lying excited states of the deuteron to feed either the singlet or ground states, contaminant deuterons from sources other than direct evaporation from the compound nucleus that preferentially populate the deuteron ground state could lower the inferred d^*/d temperature. Preliminary calculations of the contaminant deuteron emission from heavy fragments ($3\le Z\le11$) emitted from the ^{43}Sc compound system suggest that the sequential emission is dominated by the first deuteron-unbound excited state in ^{6}Li. In fact, about 60% of the total contamination results from this one state. Its production cross section (extracted from the $d\alpha$ coincidence data) is 14.6 ± 1.2 mb/sr at $\Theta_{lab}=45°$, from which we deduce a sequential emission contamination of 24 mb/sr in the deuteron yield and a modified d^*/d temperature of 1.6 ± 0.3 MeV, which is still much lower than the expected 4.4 MeV. This result is in contrast with the recent conclusions of Lee *et al.*,[22] who obtain agreement with Fermi-gas-model temperatures from population ratios of $A=7$ and 10 fragments emitted in ^{40}Ar+^{12}C collisions at $E/A=8$, 10, and 12 MeV/A, after correcting for sequential emission. To reconcile the d^*/d temperature with the Fermi-gas-model result would require an additional deuteron contamination of 30 mb/sr, beyond the sequential emission component. Such deuterons could come from direct or other noncompound reactions, but based upon the (unpublished) deuteron c.m. angular distribution measured during the experiments of Ref. 5,

we estimate less than 10 mb/sr of the deuteron yield at $\Theta_{lab}=45°$ is due to nonisotropic emission in the compound nuclear c.m. reference frame.

We have presented, for the first time, correlation functions for neutron–charged-particle coincidences, which show clear effects due to the nuclear interaction between the emitted particles. Strong correlations due to d^* and ^{5}He emission were observed in the *np* and *nα* data, and production cross sections for these unstable states were extracted. An anticorrelation due to a nuclear interaction not involving short-lived resonant states was observed in the *nd* case. It will be of interest to see if this latter effect can be explained by, e.g., formation of ^{3}H via coalescence of low-relative-momentum particles, or if it is a manifestation of quantum statistics. Finally, a nuclear temperature of 1.6 ± 0.3 MeV was deduced from the ratio of d^*/d production within the thermal model, after correction for sequential feeding. This is much lower than either the slope temperatures computed from the energy spectra of the measured light particles or the temperature expected within the Fermi-gas model, and raises again the possibility that excited-state populations may not be described by simple Boltzmann factors.[24]

We wish to acknowledge the use of particle detectors loaned from State University of New York, Stony Brook, and the National Superconducting Cyclotron Laboratory, Michigan State University, and helpful discussions with W. G. Lynch concerning the application of the thermal model to the deuteron thermometer. This work was supported in part by the National Science Foundation under Grants No. PHY88-02279 and No. PHY89-07170 and by the William and Flora Hewlett Foundation of the Research Corporation.

[1]T. C. Awes *et al.*, Phys. Rev. Lett. **61**, 2665 (1988), and references therein.
[2]Z. Chen *et al.*, Phys. Rev. C **36**, 2297 (1987), and references therein.
[3]P. A. DeYoung *et al.*, Phys. Rev. C **39**, 128 (1989).
[4]D. Ardouin *et al.*, Nucl. Phys. **A495**, 57 (1989).
[5]P. A. DeYoung *et al.*, Phys. Rev. C **41**, 1885 (1990).
[6]S. E. Koonin, Phys. Lett. **70B**, 43 (1977).
[7]M. A. Bernstein, W. A. Friedman, and W. G. Lynch, Phys. Rev. C **29**, 132 (1984).
[8]R. Hanbury Brown and R. Q. Twiss, Nature (London) **178**, 1046 (1956).
[9]S. Pratt, Phys. Rev. C **40**, 168 (1989).
[10]H. M. Xu *et al.*, Phys. Rev. C **40**, 186 (1989), and references therein.
[11]P. A. DeYoung *et al.*, Nucl. Instrum. Methods **226**, 555 (1984).
[12]M. Gordon, Ph.D. thesis, State University of New York at Stony Brook, 1988 (unpublished).
[13]W. Zajc *et al.*, Phys. Rev. C **29**, 2173 (1984).
[14]S. Pratt (private communication).
[15]L. Tomio, T. Frederico, and A. Delfino, Phys. Rev. C **41**, 876 (1990).
[16]S. A. Sofianos, A. Papastylianos, H. Fiedeldey, and E. O. Alt, Phys. Rev. C **42**, 506 (1990).
[17]R. J. Kurtz, University of California Radiation Laboratory Internal Report No. UCR1-11339, 1964 (unpublished).
[18]R. R. Doering, Ph.D. thesis, Michigan State University, 1974 (unpublished).
[19]J. Pochodzalla *et al.*, Phys. Rev. C **35**, 1695 (1987).
[20]See Eq. (8) of Ref. 19.
[21]A. Galonsky *et al.*, Phys. Lett. B **197**, 511 (1987).
[22]J. H. Lee *et al.*, Phys. Rev. C **41**, 2406 (1990).
[23]F. Puhlhofer, Nucl. Phys. **A280**, 267 (1977).
[24]N. R. Dagdeviren, Phys. Lett. B **176**, 283 (1986).